

Experimental Analysis of Low-Velocity Impact Behaviors of Carbon Fiber Composite Laminates

X. K. Li · P. F. Liu

Submitted: 1 June 2017 / Published online: 20 September 2017
© ASM International 2017

Abstract Manufacture processing of composite laminates often leads to unequal thickness of lamina and different impact responses. However, almost all existing works neglected this problem because they considered equal thickness for each lamina. This paper aims to study the influence of unequal thickness of each lamina on the impact behaviors of composite laminates by experiments. Effects of the layup patterns and impact energy are mainly studied. Results in terms of the impact experiments of carbon fiber composite laminates show that subtle difference for the thickness of the total laminate leads to relatively large errors for the impact responses, especially for the impact force-deflection curves. Also, the ratio of absorbed energy to the impact energy increases with the specimen thickness. Therefore, the practical design of composite laminates should be taken into account this difference fully due to manufacturing.

Keywords Composite laminates · Impact experiments · Manufacturing factors

Introduction

Fiber-reinforced resin matrix composites have been widely used in many fields including airplanes, pressure vessels and new energy vehicle because of high strength and stiffness to density ratios as well as excellent designability [1–3]. However, composite structures are often subjected to

low-velocity impact loads, leading to progressive damage and decrease of the structural integrity [4–6]. There are four main failure modes for composite laminates under impact loads including matrix cracking, fiber breakage, fiber/matrix interface debonding and delamination, in which the delamination and matrix cracking are two dominating damage modes during low-velocity impact.

Because of weaker load-bearing ability of laminates in the transverse direction than in the longitudinal direction, it is important to concentrate on the transverse impact responses of laminates. Low-velocity impact tests have become an important approach to study the impact resistance and damage tolerance of composite laminates. Already, many impact experiments [7–9] have been launched to study the impact responses including the impact force-deflection responses and energy dissipation mechanisms. The main factors which affect the dynamic damage evolution behaviors of laminates include the thickness of the laminate, impact energy and layup pattern. Although the latter two factors can be easily controlled during manufacturing, the total thickness of the laminate is generally hard to control because the thickness of each lamina is very thin, e.g., 0.1–0.15 mm. Thus, what should be paid more attention to is to analyze the influence of the variation of the thickness of laminates on the impact behaviors of laminates. Unfortunately, very little research is launched to address these works.

The purpose of this paper is to study the influence of the subtle difference of the total thickness of laminates on the impact behaviors. We design and manufacture the specimens with different thickness for impact experiments. Results show that designers should not neglect the variation of thickness in most cases because the impact responses show relatively large errors.

X. K. Li · P. F. Liu (✉)
Institute of Chemical Machinery and Process Equipment, School of Energy Engineering, Zhejiang University, Hangzhou 310027, China
e-mail: pfliu@zju.edu.cn; 56691747@qq.com

Drop Weight Impact Tests

Material Specimens

T300/bismaleimide composite laminates with [45/0/-45/90]_{3s} layup pattern are used for impact tests. The subscript ‘s’ represents symmetry and the symbol ‘/’ represents delaminated interface, so each specimen includes 24 plies. The specimen geometry and dimensions are listed in Fig. 1. The thickness of each position in the specimen shows difference due to manufacturing. In order to obtain the averaged thickness of the specimen, the plate is divided into four parts (A, B, C, D), as shown in Fig. 1. Six specimens are divided into two groups: C-1 (thickness 2.55–2.65 mm) and C-2 (thickness 2.65–2.75 mm), listed in Table 1.

Impact Tests

The low-velocity impact experiments are performed by Dynatup 9200 drop weight Impact Testing Machine. The impact results such as the contact force, the deflection and the absorbed energy of the laminates are acquired. As shown in Fig. 2, the machine is consisted of a clamping

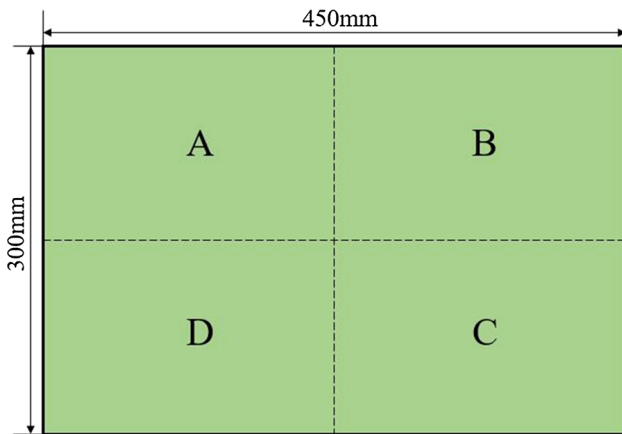


Fig. 1 Geometry and sizes for test specimens

fixture, a drop hammer device and a data acquisition system. The mass and diameter of the impactor are 5.7 kg and 16 mm, respectively.

Experiments refers to the “Standard Test Method for Measuring the Damage Resistance of a Fiber-Reinforced Polymer Matrix Composite to a Drop-Weight Impact Event” issued by the American Society for Testing and Materials (ASTM) [10]. The impact energy is calculated as

$$E = C_E h \tag{Eq 1}$$

where $C_E = 6.7 \text{ J/mm}$ is the specified ratio of the impact energy to the specimen thickness, h is the nominal thickness of specimen.

The drop height of the impactor required to produce the specified impact energy is

$$H = \frac{E}{m_d g} \tag{Eq 2}$$

where m_d is the mass of the impactor, $g = 9.8 \text{ m/s}^2$ is the acceleration due to gravity. The impact energy and height see Table 1.

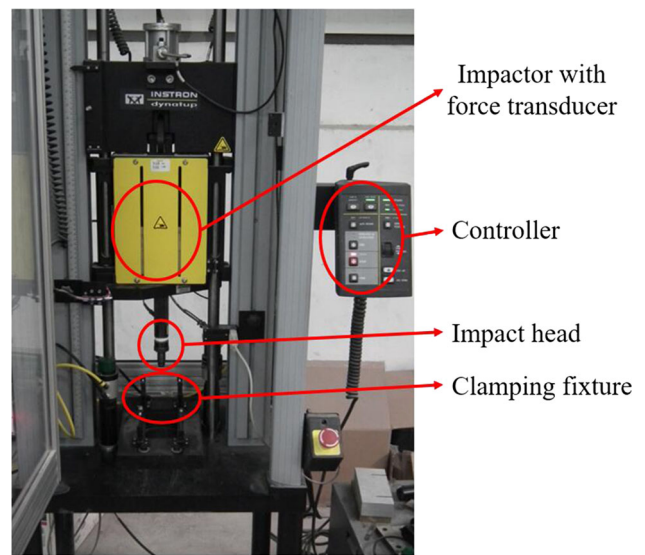


Fig. 2 Dynatup 9200 drop weight impact test machine

Table 1 Total thickness and drop height of the specimens

Specimen	Thickness at A (mm)	Thickness at B (mm)	Thickness at C (mm)	Thickness at D (mm)	Average thickness (mm)	Impact energy (J)	Drop height (mm)
C-1-1	2.69	2.73	2.80	2.79	2.75	18.4	329.0
C-1-2	2.63	2.61	2.75	2.75	2.69	18.0	321.9
C-1-3	2.80	2.75	2.68	2.69	2.73	18.3	327.3
C-2-1	2.53	2.50	2.59	2.61	2.56	17.1	305.8
C-2-2	2.65	2.63	2.58	2.54	2.60	17.4	311.2
C-2-3	2.75	2.75	2.34	2.39	2.56	17.1	305.8

The absorbed energy E_a during impact is calculated as

$$E_a(t) = m_d \frac{v_i^2 - v(t)^2}{2} + m_d g [s_i - s(t)] \quad (\text{Eq 3})$$

where v_i and s_i are the impactor velocity and the displacement at the start of contact with the target, $v(t)$ and $s(t)$ are the impactor velocity and the displacement at time t .

When the test starts, the drop hammer device will drop from a predetermined height and the steel hemispherical impactor will hit the center of the specimen with the clamping fixture. During the impact process, the history of the impact force is measured by a load transducer located above the impactor. The impact velocity is recorded by a pair of photoelectric-diodes, which is attached to the base of the test machine. The displacement of the impactor is obtained by a laser detector, which is attached to the moving impact frame. In addition, an electromagnetic braking system prevents repeated impact. After impact, irreversible energy dissipation due to damage and delamination leads to the final indentation depth at the end of impact, as shown in Fig. 3b.

Results and Discussion

Figure 4 shows the deflection-time curve. Because of the nonlinear deformation of specimen, the deflection increases first rapidly and then slowly. The curves for group C-2 are

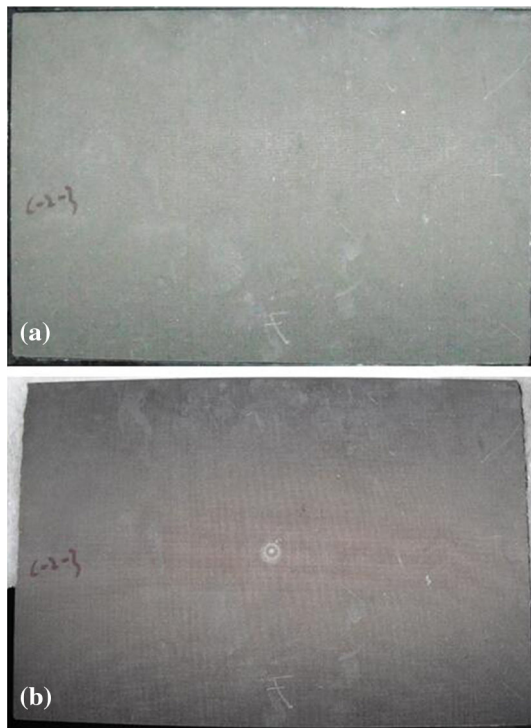


Fig. 3 The damaged specimen (a) before impact and (b) after impact

totally above those for group C-1, which shows the bending stiffness becomes smaller when the thickness decreases [11]. During impact tests, the tension stress on the lower surface is the maximum when the central area of laminates is subjected to the concentrated force impact. Matrix tension damage appears initially at the bottom of the laminate due to large bending stress. Because the tensile stress spreads in the form of stress wave, matrix cracks expand along the thickness direction from the back side to the impact side [12]. By comparison, matrix compression damage appears mainly at the upper plies. In general, matrix tension damage is dominating compared with matrix compression damage [13, 14]. Fiber breakage also appears both at the upper and bottom plies of the laminate due to large compressive and tensile stresses, respectively [13, 15]. In all specimens, delamination was clearly visible on the lower surface. Delamination crack propagates among the internal plies of laminates, which may arise from large transverse shear forces over there, consistent with the experimental phenomena observed by Johnson et al. [15]. The extent of the severe delamination always locates at the lowermost interface.

The impact contact force is an important parameter in the analysis of low-velocity impact [2], and the contact force history can be obtained by a data acquisition system. The contact force-deflection curves of laminates are mountain-like shapes shown in Fig. 5, which can be divided into two stages. At first, the impact force-deflection curves increase sharply. Later, sudden force drop and subsequent high-amplitude oscillation appear at the deflection about 3 mm, as shown in Fig. 5. This indicates large plastic deformation (the indentation on the top surface) and delamination initiation at the impact contact area, similar to some experimental results [16–19]. When the contact force reaches the maximum, it then decreases with

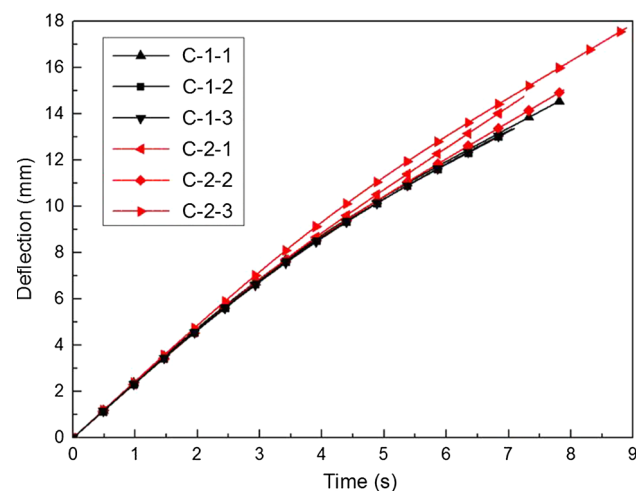


Fig. 4 The deflection-time curves during impact

the increase of deflection, where the impact curves become smooth. The total loads for group C-1 are larger than those for group C-2, which shows that increasing thickness enhances the load-bearing ability [11]. Compared with other specimens, the peak values for the impact force for the specimens C-1-1 and C-1-3 appear more early and they also show a more distinct drop in the stiffness, as shown in Fig. 5. This implies a momentary loss of contact between the impactor and specimen due to a serious bending fracture of fibers at the bottom of the specimen [12, 16, 20]. Table 2 lists the maximum loads and deflections of the specimens. By comparing with group C-1, the maximum deflection and the corresponding loads for group C-2 are higher. Most of the maximum deflection is within 15 mm, but the maximum value 17.7 mm for the specimen C-2-3 is much larger than others, which may arise from severe thickness variation for the specimen C-2-3.

Figure 6 shows the absorbed energy-deflection curves. The absorbed energy is the energy that the impact head transforms to specimens, which can be calculated from Eq 3. When the impactor starts to contact with the laminate, the energy transformation appears and the laminate deforms by absorbing the kinetic energy of the impactor. The kinetic energy has been transformed partly into the

strain energy and partly into the dissipated energy caused by the damage of composites and the frictional contact. As shown in Fig. 6, the curve slope first increases and then decreases, consistent with the change of the contact force in Fig. 5. The curves for C-1 specimens are generally above those for C-2 specimens, indicating the absorbed energy will increase with the specimen thickness. For C-1-1 and C-1-3 specimens, the absorbed energy is larger than other specimens at the beginning of impact. This is because C-1-1 and C-1-3 specimens undergo more severe fiber fracture as mentioned before, and more energy is dissipated in breaking the fibers [20]. Table 3 lists the absorbed energy by specimens. As for the absorbed energy at the maximum contact force, they are basically the same for the C-1 and C-2 specimens. Because the velocity of impact head still exists while the specimens delaminate completely, the impact energy cannot be absorbed by the specimens completely. For all specimens, the absorbed energy is lower than the impact energy. For the C-1 specimens, the ratio of the absorbed energy to the impact energy is $11.7 \text{ J}/18.2 \text{ J} = 64.3\%$; for the C-2 specimens, the ratio of the absorbed energy to the impact energy is $9.6 \text{ J}/17.2 \text{ J} = 55.8\%$. This indicates the ratio increases with the specimen thickness.

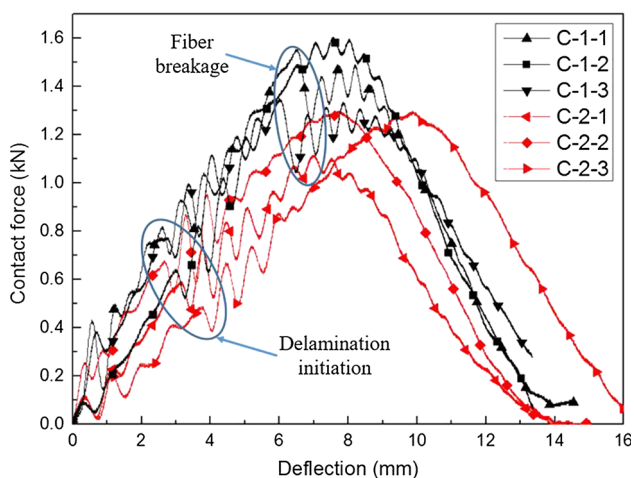


Fig. 5 The contact force-deflection curves during impact

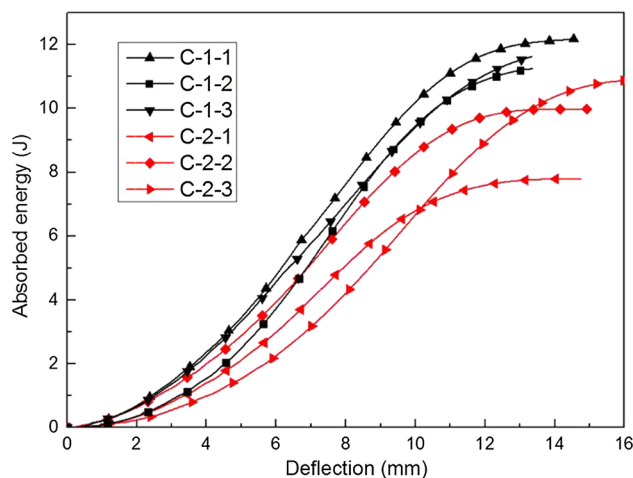


Fig. 6 The absorbed energy-deflection curves during impact

Table 2 Maximum load and deflection of the specimens

Specimen	C-1-1	C-1-2	C-1-3	C-2-1	C-2-2	C-2-3	The average value of C-1	The average value of C-2
The maximal deflection (mm)	14.6	13.4	13.3	14.8	15.0	17.7	13.8	15.8
The maximal impact load (N)	1553.4	1607.4	1351.0	1114.3	1299.1	1300.4	1503.9	1237.9
The deflection at maximal load (mm)	6.5	7.6	6.0	7.0	7.8	9.9	6.7	8.2

Table 3 Absorbed energy and impact energy for the specimens

Specimen	C-1-1	C-1-2	C-1-3	C-2-1	C-2-2	C-2-3	The average value of C-1	The average value of C-2
The maximal absorbed energy (J)	12.2	11.2	11.6	7.8	10.9	10.0	11.7	9.6
The absorbed energy at maximal load (J)	5.5	6.1	4.6	4.0	6.5	6.0	5.4	5.5
The impact energy (J)	18.4	18.0	18.3	17.1	17.4	17.1	18.2	17.2

Conclusions

This paper launches impact experiments on carbon fiber composite laminates. The main purpose is to study the influence of the thickness variation for six specimens on the transverse impact responses. From the data analysis, the following conclusions are obtained:

1. When the thickness of the specimens becomes thinner, the bending stiffness becomes smaller, deflection adds, the contact force and the absorbed energy becomes smaller. The ratio of absorbed energy to the impact energy also increases with the specimen thickness.
2. The contact force-deflection curves of laminates are mountain-like shapes. Severe plastic deformation and delamination lead to sudden force drop and high-amplitude oscillation. Subtle difference for the thickness of the total laminate leads to relatively large errors for the impact responses, especially for the impact force-deflection curves
3. During impact, matrix cracking and delamination are dominating modes. However, fiber breakage leads to a distinct drop in the stiffness of the contact force-deflection curves, and more energy is dissipated in breaking the fibers.

References

1. M. Aktas, C. Atas, B.M. Icten, R. Karakuzu, An experimental investigation of the impact response of composite laminates. *Compos. Struct.* **87**(4), 307–313 (2009)
2. C. Atas, O. Sayman, An overall view on impact response of woven fabric composite plates. *Compos. Struct.* **82**(3), 336–345 (2008)
3. Z. Aslan, R. Karakuzu, B. Okutan, The response of laminated composite plates under low-velocity impact loading. *Compos. Struct.* **59**(PII S0263-8223(02)00185-X1), 119–127 (2003)
4. E. Sevkat, B. Liaw, F. Delale, Drop-weight impact response of hybrid composites impacted by impactor of various geometries. *Mater. Des.* **52**, 67–77 (2013)
5. M. de Moura, A.T. Marques, Prediction of low velocity impact damage in carbon-epoxy laminates. *Compos. Part A Appl. Sci. Manuf.* **33**(3), 361–368 (2002)
6. G. Davies, X. Zhang, Impact damage prediction in carbon composite structures. *Int. J. Impact Eng.* **16**(1), 149–170 (1995)
7. S. Pappada, R. Rametta, A. Largo, A. Maffezzoli, Low-velocity impact response in composite plates embedding shape memory alloy wires. *Polym. Compos.* **33**(5), 655–664 (2012)
8. H. Lei, Z. Wang, L. Tong, X. Tang, Macroscopic mechanical characterization of SMAs fiber-reinforced hybrid composite under uniaxial loading. *J. Mater. Eng. Perform.* **22**(10), 3055–3062 (2013)
9. M. Sayer, N.B. Bektas, O. Sayman, An experimental investigation on the impact behavior of hybrid composite plates. *Compos. Struct.* **92**(5), 1256–1262 (2010)
10. Standard test method for measuring the damage resistance of a fibre reinforced polymer matrix composite to a drop-weight impact event, ASTM D 7136/D 7136M-05 (2005)
11. L.S. Kistler, A.M. Waas, Experiment and analysis on the response of curved laminated composite panels subjected to low velocity impact. *Int. J. Impact Eng.* **21**(9), 711–736 (1998)
12. M. Sun, Z.Q. Wang, B. Yang, X.K. Sun, Experimental investigation of GF/epoxy laminates with different SMAs positions subjected to low-velocity impact. *Compos. Struct.* **171**, 170–184 (2017)
13. E. Kim, M. Rim, I. Lee, T. Hwang, Composite damage model based on continuum damage mechanics and low velocity impact analysis of composite plates. *Compos. Struct.* **95**, 123–134 (2013)
14. A. Faggiani, B.G. Falzon, Predicting low-velocity impact damage on a stiffened composite panel. *Compos. Part A Appl. Sci. Manuf.* **41**(6), 737–749 (2010)
15. H.E. Johnson, L.A. Louca, S. Mouring, A.S. Fallah, Modelling impact damage in marine composite panels. *Int. J. Impact Eng.* **36**(1), 25–39 (2009)
16. C.S. Lopes, O. Seresta, Y. Coquet, Z. Gurdal, P.P. Camanho, B. Thuis, Low-velocity impact damage on dispersed stacking sequence laminates. Part I: experiments. *Compos. Sci. Technol.* **69**(7–8), 926–936 (2009)
17. F. Aymerich, C. Pani, P. Priolo, Damage response of stitched cross-ply laminates under impact loadings. *Eng. Fract. Mech.* **74**(4), 500–514 (2007)
18. F. Aymerich, C. Pani, P. Priolo, Effect of stitching on the low-velocity impact response of [0(3)/90(3)](s) graphite/epoxy laminates. *Compos. Part A Appl. Sci. Manuf.* **38**(4), 1174–1182 (2007)
19. F. Aymerich, F. Dore, P. Priolo, Prediction of impact-induced delamination in cross-ply composite laminates using cohesive interface elements. *Compos. Sci. Technol.* **68**(12SI), 2383–2390 (2008)
20. D. Ghelli, G. Minak, Low velocity impact and compression after impact tests on thin carbon/epoxy laminates. *Compos. Part B Eng.* **42**(7), 2067–2079 (2011)